Applied Mathematics and Computation 347 (2019) 616–630

Contents lists available at ScienceDirect

Applied Mathematics and Computation

journal homepage: www.elsevier.com/locate/amc

Effects of climate change on *Plasmodium vivax* malaria transmission dynamics: A mathematical modeling approach

Jung Eun Kim, Yongin Choi, Chang Hyeong Lee*

Department of Mathematical Sciences, Ulsan National Institute of Science and Technology (UNIST), Ulsan, Republic of Korea

ARTICLE INFO

MSC:
92D25
92D30
93A30

Keywords:
Epidemic dynamics
Plasmodium vivax malaria
Climate change
Control measures

ABSTRACT

Malaria is a major public health concern and an economic burden around the world. Currently, malaria has been declared as endemic in 91 countries. Every year more than 200 million cases of malaria are reported and more than US$2 billion has been invested in malaria control. Recent climate change caused by global warming has affected the pattern of malaria outbreak and expanded the endemic regions. In this study, we develop a malaria transmission model associated with climate-dependent parameters. We analyze the impact of climate change on malaria transmission using climate data based on Representative Concentration Pathways (RCP) scenarios. We investigate the potential risk of malaria outbreaks through the computation of seasonal reproduction number and vectorial capacity under RCP scenarios and perform a sensitivity analysis of the model parameters. Our region of focus is the northern part of South Korea where *Plasmodium vivax* malaria is currently endemic. Our results show that climate change will increase the risk of massive malaria outbreaks in the area. Furthermore, based on the actual incidence data, we estimate the parameter values that reflect the level of controls implemented recently in Korea. We found that the current level of controls is not sufficient to mitigate the effect of climate change on malaria outbreaks and a combination of stronger control measures such as at least a 10% increase of control for humans combined with a 5% increase of control for adult mosquitoes should be implemented to reduce the risk of malaria outbreaks.

© 2018 Elsevier Inc. All rights reserved.

1. Introduction

Malaria is a mosquito-borne disease transmitted by a female *Anopheles* mosquito. Malaria infection is caused by the parasites of genus *Plasmodium*. To sustain its life cycle, the parasite needs two hosts, the female *Anopheles* mosquito and humans. Malaria infection occurs predominantly in tropical countries, and many incidence cases also occur in subtropical and temperate countries. In 2016, there were 216 million incidences of malaria and 445,000 of fatalities around the world, most of whom were children aged under 5 years. In the same year, about US$2.7 billion was invested in malaria control [1].

In South Korea, located in a temperate climate zone, malaria has been prevalent for many centuries, and the primary pathogen of malaria in Korea is *Plasmodium vivax* (*P. vivax*). In 1979, South Korea was declared to be malaria-free [2], and there were no reported infection cases between 1985 and 1992. However, malaria reemerged in 1993 after one military service person was infected. Since then, South Korea, especially the northern region near the demilitarized zone (DMZ), which forms the area approximately 250 km long and 4 km wide on the border between South Korea and North Korea, has

* Corresponding author.
E-mail address: chlee@unist.ac.kr (C.H. Lee).

https://doi.org/10.1016/j.amc.2018.11.001
0096-3003/© 2018 Elsevier Inc. All rights reserved.

been an endemic area for malaria despite control efforts. Thousands of infected cases were reported every year between 1997 and 2010, and the annual cumulative incidence (CI) has decreased to hundreds after 2011 due to the intensive control policies implemented by the government for the infectious vectors and humans. *P. vivax* malaria infection is known to be benign and less severe than the *Plasmodium falciparum* malaria infection prevalent in tropical regions. However, recent research has shown that the clinical symptoms of *P. vivax* malaria infection can be very severe, even fatal [3,4], and thus a massive *P. vivax* malaria outbreak may cause considerable public health costs.

It is known that the life cycles of malaria mosquitoes and parasites are strongly affected by climate factors such as temperature and precipitation [5–8]. Climate factors have a major effect on malaria transmission in temperate areas including Korea [9]. Moreover, the optimal temperature for malaria transmission is around 25°C [10], which suggests that malaria transmission may occur predominantly between summer and early fall in Korea. It has been reported that there will be 50 million new malaria infections by the year 2100 around the world owing to climate change [11]. In the case of Korea, its climate has been gradually shifting toward a subtropical climate, which may increase the risk of massive malaria outbreaks. Thus, the investigation of the potential effect of climate change on *P. vivax* malaria transmission in Korea through a modeling study is important.

There have been many researches on mathematical modeling and analysis for malaria transmission. An ordinary differential equation model was presented, using a susceptible–exposed–infectious–recovered (SEIR) model for humans and an SEI model for adult mosquitoes and it has been shown that the transcritical bifurcation at the basic reproduction number $R_0 = 1$ is forward in the absence of malaria-induced death, while a backward bifurcation can occur at $R_0 = 1$ for larger values of the malaria-induced death rate [12]. Recently, a mathematical model of malaria transmission has been developed with a periodic biting rate of female mosquitoes and two groups (non-immune and semi-immune groups) of human population and the stability of disease-free equilibrium has been analyzed for the model [13]. In [14], the authors have proposed a malaria transmission model, using the infection age of human population and nonlinear incidence rate for transmission from vector to human and it has been shown that the infection age and nonlinear incidence rate can affect the values of the endemic steady state as well as R_0. For mathematical modeling studies on malaria transmission in Korea, the effect of zooprophylaxis as a control measure for *P. vivax* malaria transmission in Korea was investigated, using an SEIS model without morbidity [2]. An optimal control strategy for *P. vivax* malaria transmission was studied to conclude that mosquito-reduction strategies are more effective than human protection in many cases [15]. A hierarchical generalized linear model was used in [16] to study *P. vivax* malaria transmission patterns in Korea. An extensive review of the mathematical modeling of malaria transmission has been done in [17].

Concerning mathematical modeling studies on the effects of climate factors on malaria transmission, several works have been done recently. A malaria transmission model with climate-dependent parameters was developed [18]. The effect of temperature on the development and biting frequency of the malaria parasite was investigated in [19] and a delayed differential equation model with temperature-dependent parameters was developed in [20]. The effect of mortality calculation on the dynamics of malaria transmission was investigated, using temperature-dependent mortality models [21]. More recently, a deterministic age-structured malaria transmission model has been developed to assess the impact of temperature and rainfall variability [22], and a non-autonomous mathematical model has been developed to investigate the effect of both temperature and rainfall on the dynamics of mosquito population [23]. In [24], delay differential equations have been designed with temperature-dependent parameters to assess the impacts of temperature fluctuations on the mosquito population. A recent review about various mathematical models of malaria transmission dynamics associated with climate change can be found in [25].

In this paper, we develop a *P. vivax* malaria transmission model associated with climate-dependent parameters. The parameters are estimated from the previous literature and actual data, and climate data are based on Representative Concentration Pathways (RCP) scenarios [26]. Our model simulation focuses on malaria transmission in Yeoncheon, which is in the northernmost part of South Korea. Yeoncheon is adjacent to the DMZ and is currently in a malaria endemic state. Moreover, about 30% of malaria incidence cases in South Korea are military personnel [27], and Yeoncheon hosts many military units. Thus, there is a high probability that malaria incidence in Yeoncheon will grow in the future owing to climate change.

The outline of this paper is as follows; in Section 2, we present a *P. vivax* malaria transmission model associated with climate-dependent and climate-independent parameters, which are estimated by using previous articles and actual data. We also compute the seasonal reproduction number for the model by employing the method of the next generation matrix. In Section 3, we study the impact of climate change on malaria transmission with temperature and precipitation data based on RCP scenarios in Yeoncheon. Furthermore, we estimate the parameter values for malaria control from actual incidence data in Yeoncheon and investigate the effect of the controls on immature and adult mosquitoes and humans.

2. Malaria transmission model

2.1. Mathematical model

In this section, we develop a *P. vivax* malaria transmission model using a system of nonlinear differential equations. A schematic diagram of the model is given in Fig. 1. The model includes immature mosquitoes in an aquatic stage (A), female adult mosquitoes (susceptible (S_v) and infectious (I_v)), and humans (susceptible (S_h), infected and not infectious (E_h^s, E_h^l), infectious (I_h), and carrying hypnozoites (L_h)). One of the most important characteristics of *P. vivax* malaria infection of

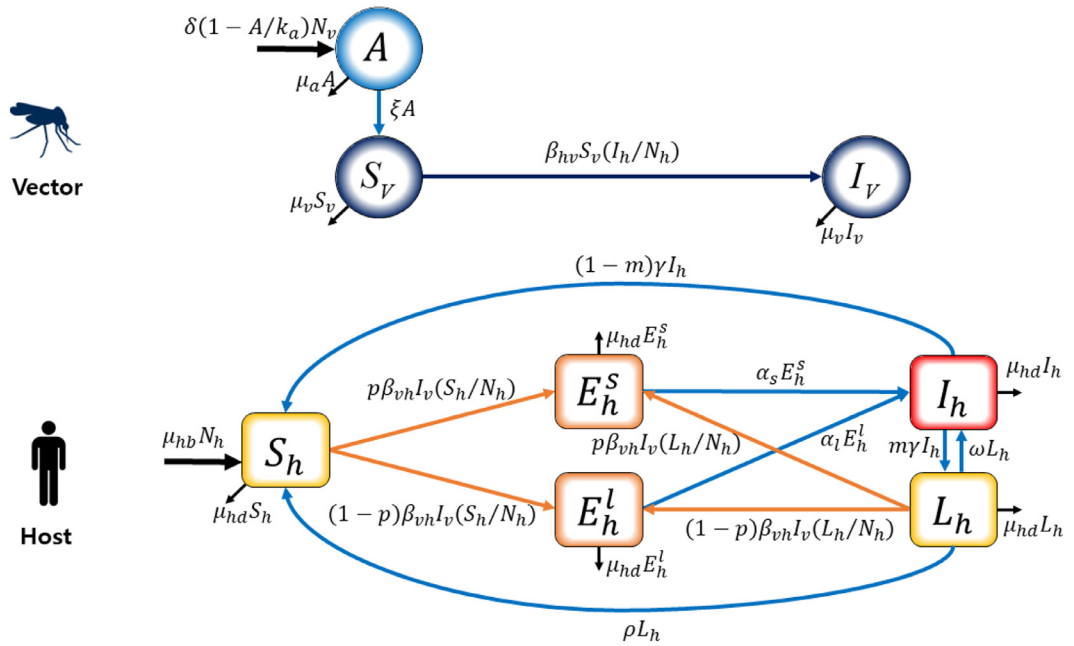

Fig. 1. *P. vivax* malaria transmission model.

humans is that there are two different incubation periods: short term and long term [2,28]. The short term and long term incubation periods are estimated as 25.9 days and 360.3 days, respectively [2,28]. Thus, the long term incubation period is about 14 times longer than the short term incubation period. It is known that the time scale difference between the two incubation periods can affect the *P. vivax* malaria transmission dynamics over the years and in particular, individuals in long-term incubation period during a year may trigger a malaria outbreak in the next year [29,30]. In the model, E_h^s and E_h^l denote the exposed (or latent) states with short-term and long-term incubation period, respectively.

The governing equation of the model can be written as follows:

$$\begin{aligned}
\frac{dA}{dt} &= \delta\left(1-\frac{A}{k_a}\right)N_v - \xi A - \mu_a A \\
\frac{dS_v}{dt} &= \xi A - \beta_{hv} S_v I_h/N_h - \mu_v S_v \\
\frac{dI_v}{dt} &= \beta_{hv} S_v I_h/N_h - \mu_v I_v \\
\frac{dS_h}{dt} &= \mu_{hb} N_h + (1-m)\gamma I_h + \rho L_h - \beta_{vh} S_h I_v/N_h - \mu_{hd} S_h \\
\frac{dE_h^s}{dt} &= p\beta_{vh} I_v (S_h + L_h)/N_h - \alpha_s E_h^s - \mu_{hd} E_h^s \\
\frac{dE_h^l}{dt} &= (1-p)\beta_{vh} I_v (S_h + L_h)/N_h - \alpha_l E_h^l - \mu_{hd} E_h^l \\
\frac{dI_h}{dt} &= \alpha_s E_h^s + \alpha_l E_h^l + \omega L_h - \gamma I_h - \mu_{hd} I_h \\
\frac{dL_h}{dt} &= m\gamma I_h - \omega L_h - \rho L_h - \beta_{vh} L_h I_v/N_h - \mu_{hd} L_h
\end{aligned} \tag{1}$$

where $N_v = S_v + I_v$ and $N_h = S_h + E_h^s + E_h^l + I_h + L_h$.

In the system (1), δ denotes the per capita egg deposition rate of female adult mosquitoes, ξ denotes the maturation rate of immature mosquitoes, k_a is a carrying capacity for the immature mosquitoes, and μ_a and μ_v refer to the per capita death rates of the immature mosquitoes and adult mosquitos, respectively. We use β_{hv} and β_{vh} to denote the transmissible rates from human to vector and from vector to human, respectively, and use α_s (α_l) to denote the per capita rate of progression of humans from the short-term (long-term) exposed state to the infectious state. We use γ to denote the recovery rate from the infectious state and m to denote the probability of carrying hypnozoites after recovery from the infectious state. Here ρ is the per capita rate of loss of hypnozoites for humans, p is the probability of exposed humans going through short-term incubation periods, and ω is the progression rate from L_h to I_h due to the relapse to infectious state, i.e. $1/\omega$ is the average

Table 1
Descriptions and values of parameters.

Symbol	Description	Value	Reference
k_a	Vector carrying capacity	45510×5	[22]
b_v	Probability of infection from infected humans to susceptible mosquitoes	0.049	Estimated
b_h	Probability of malaria transmission from infected mosquitoes to human	0.334	Estimated
$1/\alpha_s$	Short-term latent period for human (days)	25.9	[2,28]
$1/\alpha_l$	Long-term latent period for human (days)	360.3	[2,28]
$1/\gamma$	Infectious period for human (days)	14	[2]
μ_{hb}	Human birth rate (day^{-1})	2.2098×10^{-5}	[38]
p	Probability of exposed humans going through short-term incubation periods	0.25	[2,15]
$1/\rho$	Average time of carrying hypnozoites (days)	365	[35]
$1/\omega$	Average time from a primary attack to a relapse (days)	150	[35]
m	Probability of carrying hypnozoites after a complete course of treatments	0.13	[35]
δ	Per capita egg deposition rate	**	[22]
ξ	Maturation rate of immature mosquitoes	**	[22]
β_{hv}	Transmissible rate (h → v) (day^{-1})	$b(T)b_v$	[22]
β_{vh}	Transmissible rate (v → h) (day^{-1})	$b(T)b_h$	[22]
μ_a	Mortality rate of the aquatic state (day^{-1})	**	[22]
μ_v	Mortality rate of the mosquitoes (day^{-1})	**	[22]

(**Time-dependent parameters estimated in the climate-dependent parameters section.)

time from a primary attack to a relapse. Finally, μ_{hb} and μ_{hd} denote the human birth and natural death rates, respectively, and we assume that the two rates are equal throughout this paper. Here we ignore the malaria-induced death rate, since the human mortality rate by infection of P. vivax malaria in Korea is almost zero [27,31]. The detailed parameter values and descriptions are given in Section 2.3.

The basic reproduction number R_0 measures the average number of secondary infectious cases caused by one infectious individual introduced into a whole susceptible population, and it is computed by the method of the next-generation matrix [32]. When parameters in the system of model equations are time-dependent, the seasonal reproduction number R_s is used [33]. As some parameters in the system (1) are time-dependent (see Table 1), we compute the seasonal reproduction number R_s of the system (1) as follows.

Theorem 1. *The seasonal reproduction number R_s of the system (1) is*

$$R_s = \sqrt{\frac{\beta_{hv}\beta_{vh}(\rho+\omega+\mu_{hd})(\alpha^L+\alpha^S+(1-p)\alpha^L+p\alpha^S)S_v}{\left(\alpha^L+\mu_{hd}\right)\left(\alpha^S+\mu_{hd}\right)\left(\gamma(\rho+\omega-m\omega)+(\gamma+\rho+\omega)\mu_{hd}+\mu_{hd}^2\right)\mu_v N_h}}.$$

Proof. Let $\mathbf{x} = (I_v, E_h^s, E_h^l, I_h, L_h)^T$. Then we define the vector $\mathcal{F}(\mathbf{x})$ whose ith entry denotes the rate of new infections in the ith entry of the vector $\mathbf{x}$ and $\mathcal{V}(\mathbf{x})$ whose ith entry denotes the net transition rate out of the ith entry of the vector $\mathbf{x}$. Then, one can find

$$\mathcal{F}(\mathbf{x}) = \begin{pmatrix} \beta_{hv}S_vI_h/N_h \\ p\beta_{vh}I_v(S_h+L_h)/N_h \\ (1-p)\beta_{vh}I_v(S_h+L_h)/N_h \\ 0 \\ 0 \end{pmatrix}, \quad \mathcal{V}(\mathbf{x}) = \begin{pmatrix} \mu_vI_v \\ (\alpha_s+\mu_{hd})E_h^s \\ (\alpha_l+\mu_{hd})E_h^l \\ -(\alpha_sE_h^s+\alpha_lE_h^l+\omega L_h)+(\gamma+\mu_{hd})I_h \\ -m\gamma I_h+(\beta_{vh}I_v/N_h+\omega+\rho+\mu_{hd})L_h \end{pmatrix}.$$

Let F and V denote the Jacobians of $\mathcal{F}(\mathbf{x})$ and $\mathcal{V}(\mathbf{x})$ evaluated at the disease-free equilibrium, which consists of all zeros except for A, S_v, S_h, respectively. Then, one can find

$$F = \begin{bmatrix} 0 & 0 & 0 & \beta_{hv}S_v/N_h & 0 \\ p\beta_{vh} & 0 & 0 & 0 & 0 \\ (1-p)\beta_{vh} & 0 & 0 & 0 & 0 \\ 0 & 0 & 0 & 0 & 0 \\ 0 & 0 & 0 & 0 & 0 \end{bmatrix},$$

$$V = \begin{bmatrix} \mu_v & 0 & 0 & 0 & 0 \\ 0 & \alpha^S+\mu_{hd} & 0 & 0 & 0 \\ 0 & 0 & \alpha^L+\mu_{hd} & 0 & 0 \\ 0 & -\alpha^S & -\alpha^L & \gamma+\mu_{hd} & -\omega \\ 0 & 0 & 0 & -m\gamma & \omega+\rho+\mu_{hd} \end{bmatrix}.$$

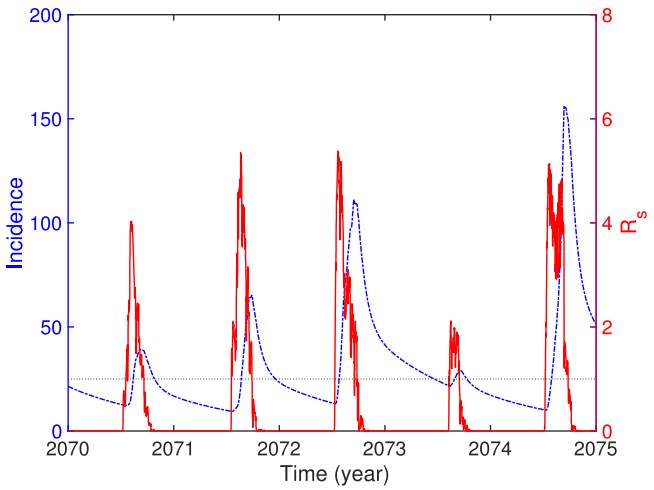

Fig. 2. Plot of the incidence of humans (blue dashed) and the seasonal reproduction number R_s (red solid) based on RCP 2.6 over 5 years. The black dotted horizontal line represents $R_s = 1$. (For interpretation of the references to color in this figure legend, the reader is referred to the web version of this article.)

Thus, one can obtain

$$FV^{-1} = \begin{bmatrix} 0 & \frac{\alpha^S(\rho+\omega+\mu_{hd})}{(\alpha^S+\mu_{hd})}C & \frac{\alpha^L(\rho+\omega+\mu_{hd})}{(\alpha^L+\mu_{hd})}C & (\rho+\omega+\mu_{hd})C & \omega C \\ \frac{p\beta_{vh}}{\mu_v} & 0 & 0 & 0 & 0 \\ \frac{(1-p)\beta_{vh}}{\mu_v} & 0 & 0 & 0 & 0 \\ 0 & 0 & 0 & 0 & 0 \\ 0 & 0 & 0 & 0 & 0 \end{bmatrix},$$

where

$$C = \frac{S_v\beta_{hv}}{N_h\left(\gamma(\rho+\omega-m\omega)+(\gamma+\rho+\omega)\mu_{hd}+\mu_{hd}^2\right)}.$$

Therefore, the seasonal reproduction number R_s, that is, the spectral radius of FV^{-1} is computed as

$$R_s = \sqrt{\frac{\beta_{hv}\beta_{vh}(\rho+\omega+\mu_{hd})(\alpha^L+\alpha^S+(1-p)\alpha^L+p\alpha^S)S_v}{\left(\alpha^L+\mu_{hd}\right)\left(\alpha^S+\mu_{hd}\right)\left(\gamma(\rho+\omega-m\omega)+(\gamma+\rho+\omega)\mu_{hd}+\mu_{hd}^2\right)\mu_v N_h}}.$$

□

Fig. 2 shows the relationship between the incidence of infectious humans and the seasonal reproduction number for 5 years after 2070. In Fig. 2, one can see that the incidence is increasing if $R_s > 1$ and decreasing if $R_s < 1$, and the peaks of the incidence occur when R_s is decreasing at $R_s = 1$. Moreover, R_s values are between 2 and 6 at the peaks between July and August, which means that the risk of malaria outbreak becomes very high during the summer.

2.2. Climate data under RCP scenarios

RCP scenarios were developed by the Intergovernmental Panel on Climate Change (IPCC) in 2014 [26]. We utilize the daily climate data provided by the Korea Meteorological Administration (KMA) under four representative scenarios: the lowest forcing level scenario (RCP 2.6), the two medium level scenarios (RCP 4.5/6.0), and the high-level scenario (RCP 8.5) [34].

Fig. 3 shows the 5-year averages of daily temperature and precipitation in Yeoncheon from year 2020 to 2099. The average daily temperature tends to increase over 80 years, and in particular, in the case of RCP 8.5, the average temperature will increase by more than 4°C in this period. On the other hand, the average daily precipitation fluctuates under all four RCP scenarios. These facts may affect the population size of mosquitoes and the pattern of malaria outbreak. For the correlation between malaria incidence and temperature/precipitation under RCP scenarios, refer to Appendix A.

2.3. Parameter estimation

The model parameters are classified into climate-independent and climate-dependent parameters. For example, the human birth rate and death rate are climate-independent parameters. The probability m of carrying hypnozoites after a complete course of treatments has two constant values: $m = 0.13$ if a patient takes primaquine, which is a commonly-used

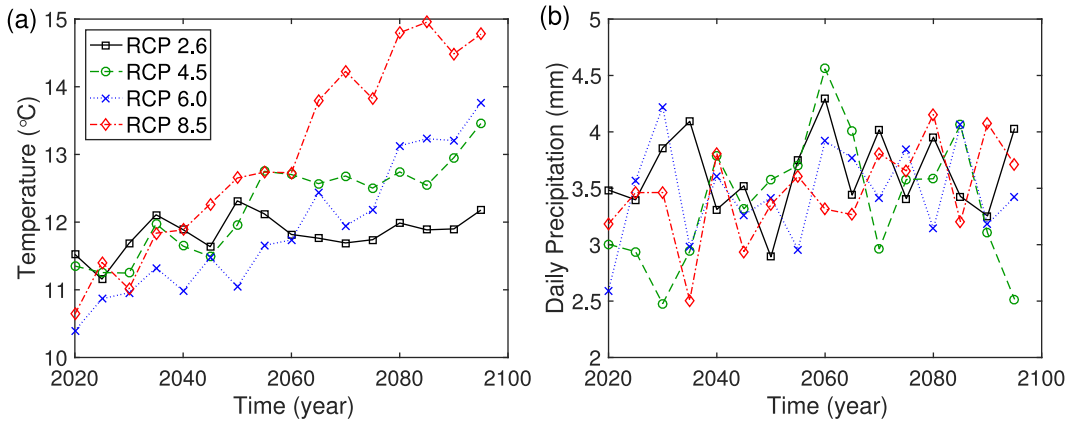

Fig. 3. Five-year average of (a) daily temperature and (b) daily precipitation from year 2020 to 2099 based on RCP 2.6, RCP 4.5, RCP 6.0, and RCP 8.5 climate change scenarios in Yeoncheon.

drug to prevent a relapse of infection; and $m = 0.68$ otherwise [35]. In South Korea, most infected patients should take primaquine [27] and thus we take $m = 0.13$. Other climate-independent parameters are described in Table 1.

The climate-dependent parameters are related to the life cycle and biting rate of mosquitoes. These parameters are described as follows.

(1) The per capita egg deposition rate δ is estimated as [22]

$$\delta(T) = \max(-0.153T^2 + 8.61T - 97.7,\ 0),$$

where T is the daily average temperature.

(2) Per capita death rates μ_a and μ_v of the immature mosquitoes and adult mosquitos, respectively, are estimated as follows [20,22]:

$$\mu_a(T) = \min\left(0.002\exp\left(\left(\frac{T-23}{6.05}\right)^2\right),\ 1\right)$$

and

$$\mu_v(T) = \max(-\ln\left(-0.000828T^2 + 0.0367T + 0.522\right),\ 0).$$

(3) The maturation rate ξ of immature mosquitoes is estimated as follows [22]:

$$\xi(T,R) = \frac{e(T)p_E(R)p_L(T,R)p_P(R)}{\tau_{EA}(T)}.$$

Here $e(T)$ is the lifetime number of eggs laid by adult mosquitoes, which can be computed as the total number $f(T)$ of eggs laid per day by a mosquito multiplied by the average adult lifespan $1/\mu_v(T)$, so that

$$e(T) = \frac{f(T)}{\mu_v(T)}, \quad \text{where } f(T) = -0.153T^2 + 8.61T - 97.7.$$

Moreover, $p_E(R), p_L(T, R)$, and $p_P(R)$ are the daily survival probabilities of eggs, larvae, and pupae, respectively, estimated as

$$p_E(R) = \frac{3.6R(R_L - R)}{R_L^2}, \quad p_L(T,R) = e^{-(0.00554T - 0.06737)}\frac{R(R_L - R)}{R_L^2}$$

and

$$p_P(R) = \frac{3R(R_L - R)}{R_L^2},$$

where R_L is the rainfall threshold given by $R_L = 50$ [36] and R is the daily rainfall amount averaged over the previous 2-week period [37]. Here $\tau_{EA}(T)$ is the total development time from egg to adult mosquito estimated by $\tau_{EA}(T) = 1/(-0.00094T^2 + 0.049T - 0.552)$.

(4) Transmissible rates β_{hv} and β_{vh} are computed as $\beta_{hv}(T) = b(T)b_v$ and $\beta_{vh}(T) = b(T)b_h$, where $b(T) = 0.000203T(T - 11.7)\sqrt{42.3 - T}$ is the biting rate [19,22]. Moreover, b_v denotes the probability of infection from infected humans to susceptible mosquitoes, and b_h denotes the probability of malaria transmission from infected mosquitoes to humans. These two parameters are estimated as $b_v = 0.049$ and $b_h = 0.334$ by fitting the data of actual incidence cases of the year 2001 in Yeoncheon.

The climate-dependent parameter functions are displayed in Fig. 4.

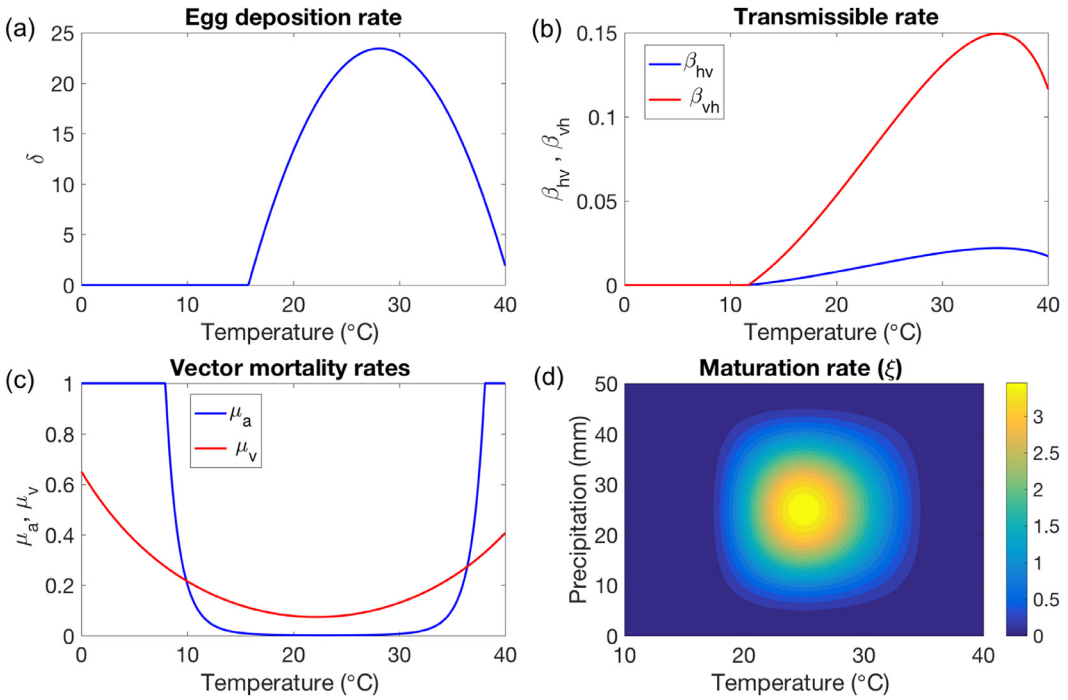

Fig. 4. Plots of (a) egg deposition rate, (b) transmissible rate, and (c) vector mortality rates versus temperature in the range of 0°C and 40°C. (d) A contour plot of the maturation rate versus the temperature and precipitation.

3. Numerical results

In this section, we investigate the climate-dependent dynamics of malaria transmission in Yeoncheon. We simulate the model (1) with the described parameter values, using climate data from Yeoncheon based on RCP 2.6, RCP 4.5, RCP 6.0, and RCP 8.5 scenarios [34]. The current total population of Yeoncheon is 45,510, and the birth rate per day is 2.2098×10^{-5} [38].

3.1. Malaria transmission dynamics based on RCP scenarios

The human incidence of malaria infection has recently decreased in South Korea following the implementation of control policies, and in particular in Yeoncheon the reported annual incidence of humans has not exceeded 10 for the last 4 years [31]. It can be expected that Yeoncheon will be malaria-free in the near future if proper control measures are maintained. To investigate the impact of climate change on malaria transmission, we assume a malaria-free state in Yeoncheon by the year 2030 and consider two cases. The first case is that infectious mosquitoes emerge through the DMZ from North Korea. In this case, we assume $I_h(0) = E_h^s(0) = E_h^I(0) = L_h(0) = 0$ and $I_v(0) = 100$ on the initial date, May 1, 2030. The second case is that there is one infected human at onset similarly to the case of reemergence in 1993 in South Korea. In this case, we assume $E_h^s(0) = E_h^I(0) = L_h(0) = I_v(0) = 0$, $I_h(0) = 1$ on May 1, 2030. In both cases, we assume $N_v(0) = N_h(0) \times 2$ [39] and $A(0) = N_h(0) \times 5$ [22].

In Fig. 5, we present the simulation results of the first case. Fig. 5 shows the time evolution of incidence and annual cumulative number of infectious mosquitoes and humans for the 70 years between 2030 and 2100 in the model without controls. Fig. 5(a) and (b) show that malaria outbreaks for mosquitoes and humans have recurrent seasonal patterns. Fig. 5(c) and (d) depict that large outbreaks for humans and mosquitoes will occur after the year 2060, especially for RCP 2.6 and RCP 4.5 scenarios. The simulation results of the second case are similar to those of the first case (refer to Appendix B).

3.2. Vectorial capacity and intensity under RCP scenarios

To investigate the potential of malaria transmission, we use the vectorial capacity (VC), which represents the potential contact rate between infectious vectors and susceptible humans [40,41]. Using the results in [17,42], we derive the explicit form of the VC in our model as

$$VC = \frac{nb^2 b_v b_h e^{-\frac{\mu_v}{\varepsilon}}}{\mu_v},$$

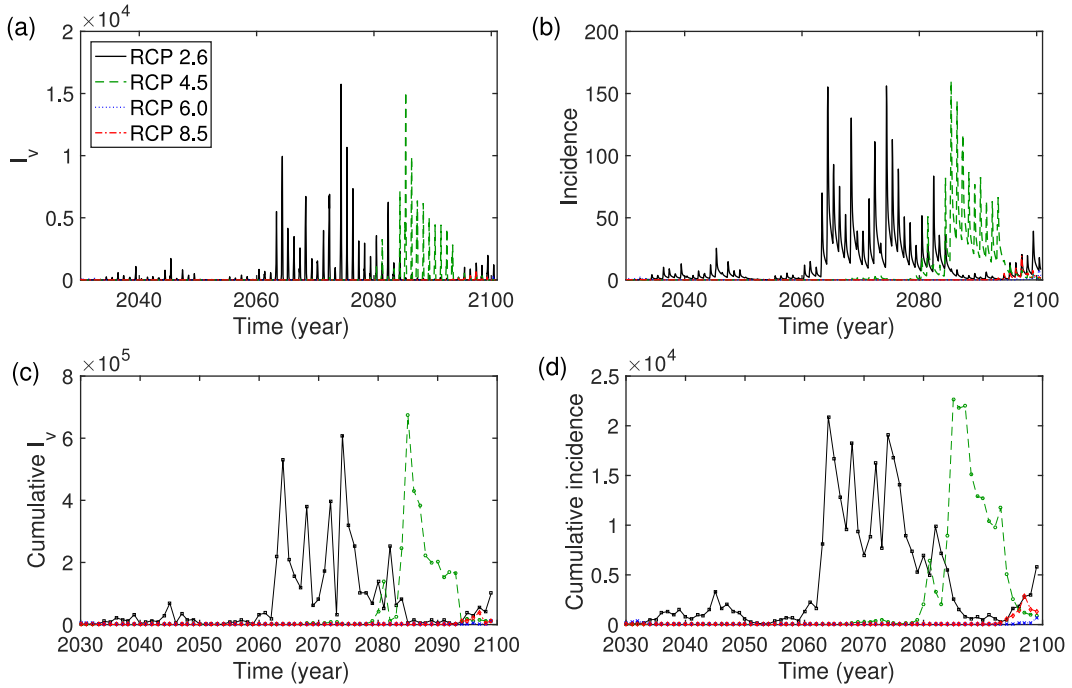

Fig. 5. Incidences of malaria infections in case of no control: Time series of (a) number of infectious mosquitoes and (b) incidence of humans, and annual cumulative number of (c) infectious mosquitoes and (d) incidence of humans are displayed during 70 years based on RCP 2.6 (black solid line), RCP 4.5 (green dashed line), RCP 6.0 (blue dotted line), and RCP 8.5 (red dash-dotted line). (For interpretation of the references to color in this figure legend, the reader is referred to the web version of this article.)

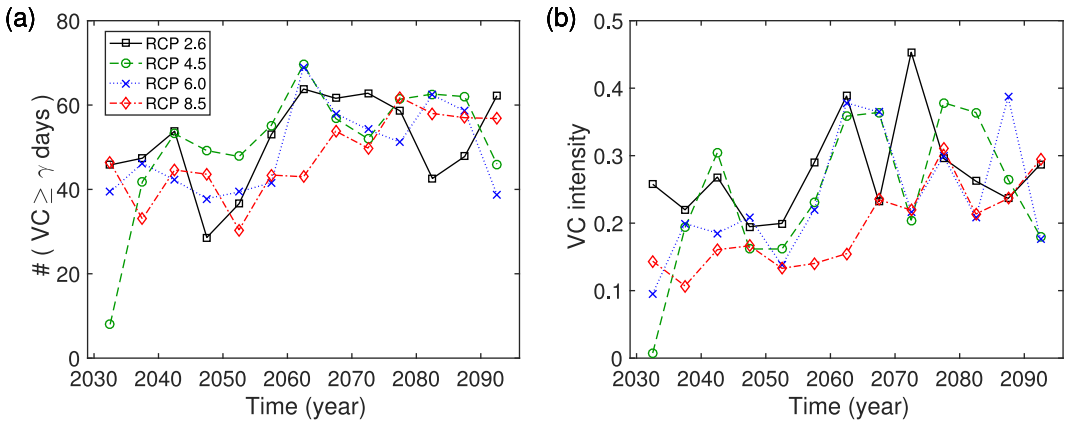

Fig. 6. Vectorial capacity (VC): (a) 5-year average of the number of days on which VC is higher than γ in each year; (b) 5-year average of VC intensity defined as the average of VC on the highest sequential 2 months in each year.

where $n = \frac{N_v}{N_h}$ is the female vector-to-human population ratio, $\varepsilon = \frac{T-14.5}{105}$ is the virus incubation rate (day^{-1}) [9], and other parameters are defined as in Table 1. As the basic reproduction number R_0 is expressed as $R_0 = \frac{VC}{\gamma}$ [43] and $R_0 = 1$ is the the critical value for the malaria outbreak, the critical value for VC is $VC = \gamma$. To investigate the changes in the potential rate of malaria outbreak caused by climate change, we consider the expected duration of epidemic risk as the number of days for which $VC \geq \gamma$ and compute the intensity of VC defined by the average of VC over the highest consecutive 2 months. Fig. 6 depicts that the VC and its intensity tend to increase over a long period of time.

3.3. The effects of human and vector controls

In this section, we investigate the effects of controls applied on vectors and humans. We first estimate the parameter values reflecting the current level of the controls implemented in Korea, using malaria incidence data between 2001 and

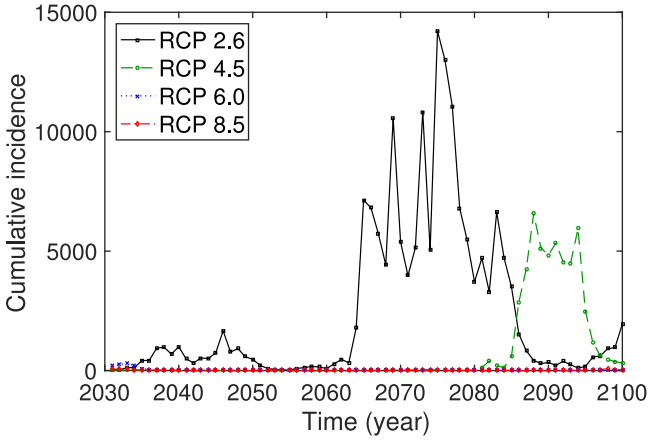

Fig. 7. CI for the control parameters $c_\beta = 0.02$, $\mu_v = 0.02$ (middle) with the initial condition $I_v(0) = 100$.

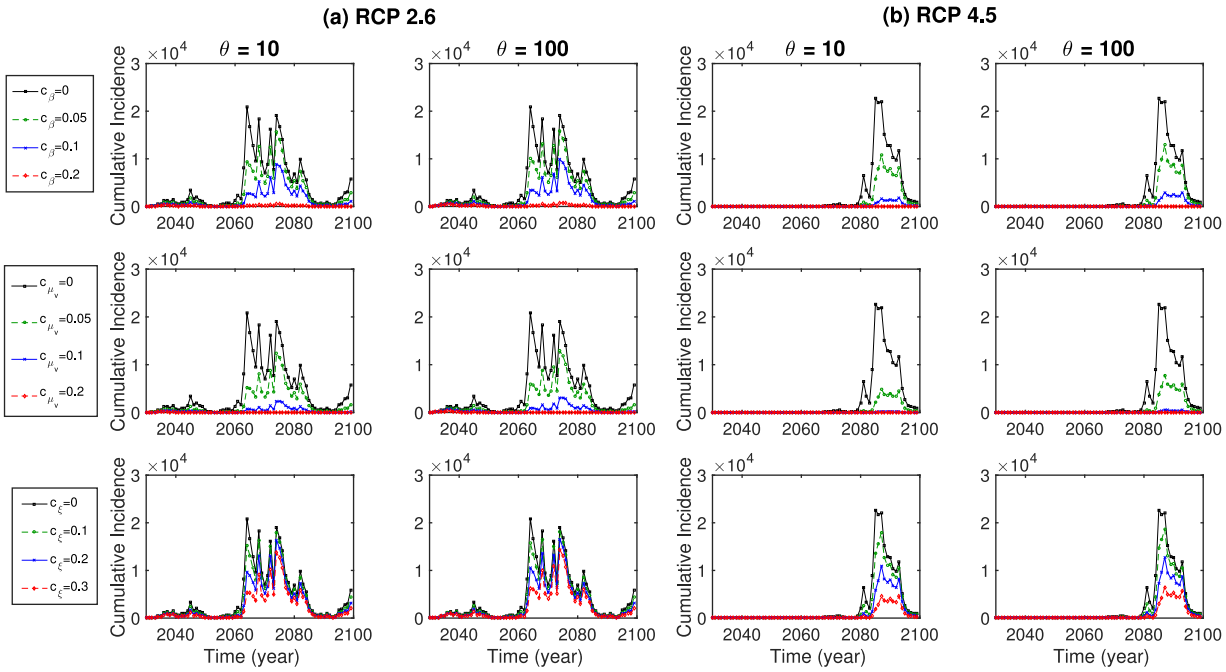

Fig. 8. Control effects on parameters β (top), μ_v (middle), and ξ (bottom) under (a) RCP 2.6 and (b) RCP 4.5 for the control threshold $\theta = 10$ or 100 with the initial condition $I_v(0) = 100$.

Table 2
Total incidence between 2030 and 2100 shown in Fig. 7.

RCP scenarios	2.6	4.5	6.0	8.5
Total incidence	167283	51265	1221	550

2017 provided by KCDC [31]. Because the controls for adult mosquitoes and humans are the two main control measures, we estimate the change in the values of the parameters β and μ_v by the controls from the incidence data during the past 17 years. The estimation reflects the fact that the control measures have been implemented mostly during the period between May and October every year in Korea [27]. Using the step size 0.01 about the values of the two parameters β and μ_v, we found that the best-fitting values for the two controls are 2% decrease of β and 2% increase of μ_v with a relative error 0.0072.

Fig. 7 and Table 2 show that if the current level of controls would be implemented from onset of the malaria transmission with $I_v(0) = 100$, it would not prevent the malaria outbreak on a long time scale, especially for the case of RCP 2.6 and RCP 4.5. Thus, in the remainder of this section, we focus on investigating the appropriate levels of controls to prevent massive

Table 3
Total CI between year 2030 and year 2100 as shown in Fig. 8.

	RCP 2.6		RCP 4.5	
	$\theta = 10$	$\theta = 100$	$\theta = 10$	$\theta = 100$
$c_\beta = 0.05$	1.9575e+5	2.0203e+5	8.1395e+4	9.4230e+4
$c_\beta = 0.1$	9.7163e+4	1.0912e+5	1.3842e+4	2.4440e+4
$c_\beta = 0.2$	7.2625e+3	1.1712e+4	1.8679e+2	5.2095e+2
$c_{\mu_v} = 0.05$	1.3941e+5	1.4907e+5	3.8741e+4	5.7863e+4
$c_{\mu_v} = 0.1$	2.6475e+4	3.6047e+4	1.4285e+3	4.5478e+3
$c_{\mu_v} = 0.2$	1.3035e+3	2.7771e+3	7.0198e+1	1.1961e+2
$c_\xi = 0.1$	2.4921e+5	2.5263e+5	1.3197e+5	1.3748e+5
$c_\xi = 0.2$	2.0066e+5	2.0790e+5	8.2004e+4	9.3458e+4
$c_\xi = 0.3$	1.5055e+5	1.6172e+5	3.7661e+4	5.0987e+4

rates of malaria transmission. In the model, we include practical control measures such as: (a) mosquito nets, mosquito repellent, preventive medicines, and quarantine for humans; (b) insecticide for adult mosquitoes; and (c) growth suppressor for immature mosquitoes in the aquatic stage [27]. We assume that these control measures are implemented in the period between May and October every year according to the current control manual in Korea [27]. In the model Eq. (1), control measure (a) can be expressed by replacing the transmissible rate β by $\beta(1 - c_\beta)$, where $c_\beta (0 \le c_\beta \le 1)$ is the reduction rate by the control measure. Similarly, control measure (b) is modeled by replacing the death rate μ_v by $\mu_v(1 + c_{\mu_v})$, where c_{μ_v} is a nonnegative number reflecting the effect of insecticide on the death of the vectors. The control measure (c) is expressed by replacing the maturation rate ξ and by $\xi(1 - c_\xi)$, where $c_\xi (0 \le c_\xi \le 1)$ is the reduction rate by the control measure.

In Fig. 8, the CI of humans is displayed using four different levels of each control for immature and adult mosquitoes and humans under RCP 2.6 and RCP 4.5 scenarios (for the cases of RCP 6.0 and RCP 8.5, refer to Appendix C). For the condition on the initiation of control measures, we consider two cases: control measures are implemented immediately when the number θ of human CI cases in one year reaches 10 and 100, respectively. In both cases, the implemented control measure will continue between May and October every year through 2100 after the day when the control measure is initiated. The simulation results in Fig. 8 show that massive outbreaks will occur if there is no control. Moreover, 5% and 10% increases of control for adult mosquitoes or humans are not sufficient to prevent a large number of infections over a long period of time. In the case of control for immature mosquitoes, even a 30% decrease on the maturation rate is not sufficiently effective at reducing the CI. For an effective control over a long period of time, at least 20% increase of one control measure for adult mosquitoes or humans is required when $\theta = 10$ or 100. Moreover, early control has a certain effect of reducing the CI. Table 3 lists the results of a comparison of total CI for the two cases of $\theta = 10$ or 100.

It is worth noting from Fig. 8 and Table 3 that the control of adult mosquitoes is the most effective approach. However, many of the infected mosquitoes move into Yeoncheon area through the DMZ from North Korea where malaria infection is endemic [16], and thus the effect of strengthening control measures for adult mosquitoes is limited as long as the border area of North Korea remains in an endemic state. Thus, a practical way of implementing effective control measures is to strengthen the control for humans while maintaining a moderate level of control for vectors.

Fig. 9 shows the effect of combined controls for vectors and humans. In Fig. 9, the simulation results suggest that at least a 10% increase of control of humans combined with a 5% increase of control for adult mosquitoes is an effective control option. Considering the current level ($c_\beta = 0.02,\ c_{\mu_v} = 0.02$) of controls, implementation of a much stronger control measure, especially for humans, is required to prevent massive malaria outbreaks in the future.

3.4. Sensitivity analysis

We perform sensitivity analysis on the model parameters described in Table 1. We utilize the normalized forward sensitivity index of the CI on the parameter p, which is defined as follows [44]:

$$CI_p = \frac{\partial(CI)}{\partial p} \times \frac{p}{(CI)}.$$

Fig. 10 displays the normalized forward sensitivity index of the CI on the constant parameters. A total of 1000 sets are randomly chosen from the uniform distribution in the range of $\pm 10\%$ of the parameter values in Table 1. One can see that γ is a negative influential parameter, whereas m, ω, p, α_s, α_l, and k_a have a positive influence on CI. In particular, α_l has a more positive influence on CI than α_s for the 5-year period.

Fig. 11 shows the change in temperature-dependent parameters under the RCP 6.0 scenario over 365 days beginning January 1, 2030. The transmissible rates β_{hv} and β_{vh} are maintained at high levels around the day 200 in the summer season. On the other hand, the mortality rates of the immature and adult mosquitoes, μ_a and μ_v, are very low during the summer season. Thus, the risk of malaria transmission is high during the summer period including June, July, and August.

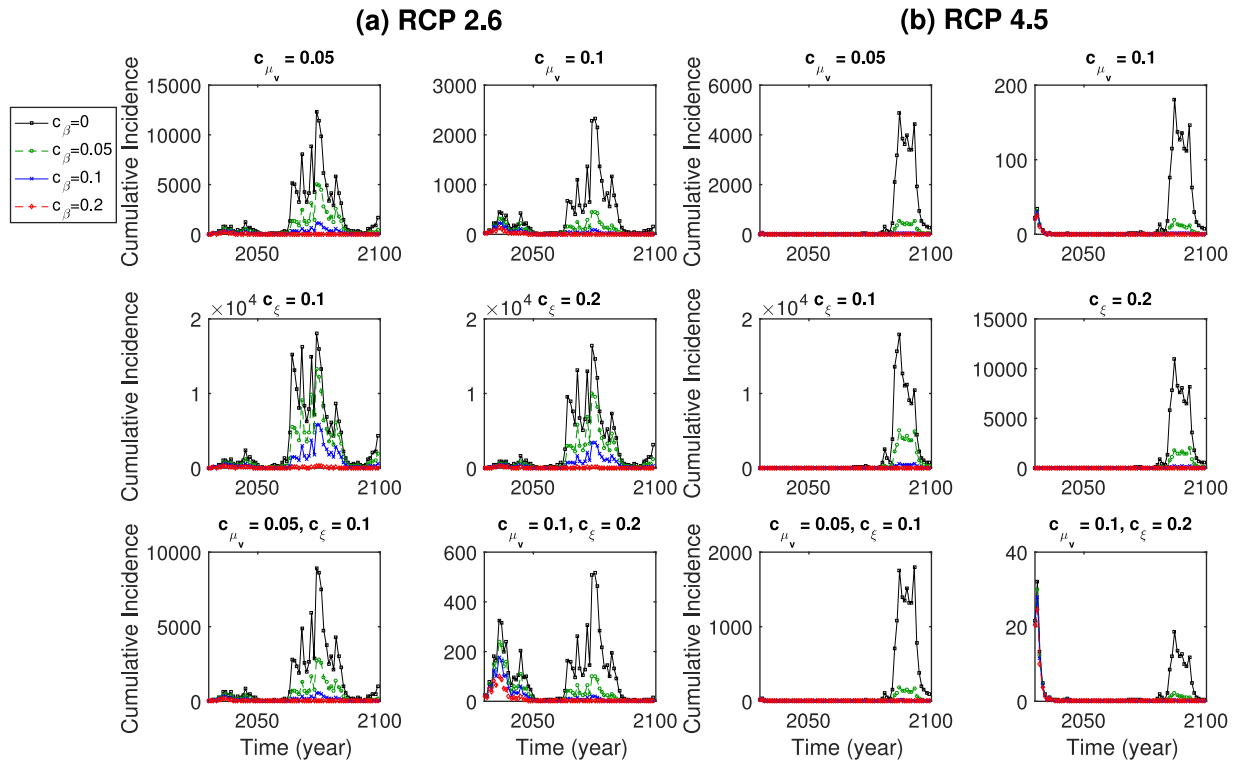

Fig. 9. Combined control effects on μ_v (top), ξ (middle), and both (bottom) with control on β under (a) RCP 2.6 and (b) RCP 4.5 for the control threshold $\theta = 10$ with $I_v(0) = 100$.

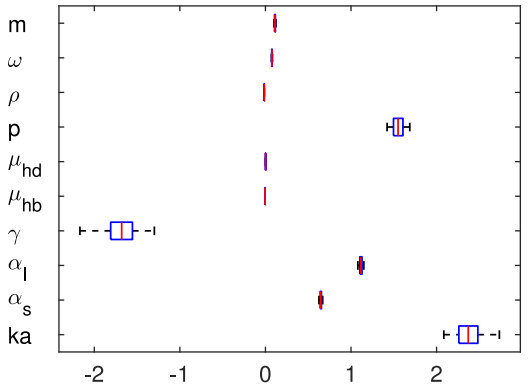

Fig. 10. Normalized forward sensitivity index of the CI of humans for the 5 years from 2030 under RCP 6.0. The initial condition as $I_h(0) = E_h^s(0) = E_h^l(0)$, $I_v(0) = 100$, $N_h(0) = 45{,}510$, and $N_v(0) = 2 \times 45{,}510$.

4. Conclusion

In this paper, we constructed a *P. vivax* malaria transmission model with climate-dependent parameters. The climate-dependent parameters were estimated from previous studies and actual data. We have studied the impact of climate change on malaria transmission dynamics under RCP scenarios in Korea. Furthermore, we have investigated the effect of controls on immature mosquitoes in the aquatic stage, adult mosquitoes, and humans.

We estimated the current control parameters values from the previous incidence data in South Korea. We have shown that if the current level of control measures continues to be implemented in the future, climate change would significantly increase the incidence of infectious humans and mosquitoes, which would be much larger than the incidence caused by the reemergence case in 1993. Moreover, the simulation results show that earlier control is more effective in reducing human incidence cases. Control of adult mosquitoes is very effective; however, it remains a challenging task as many malaria

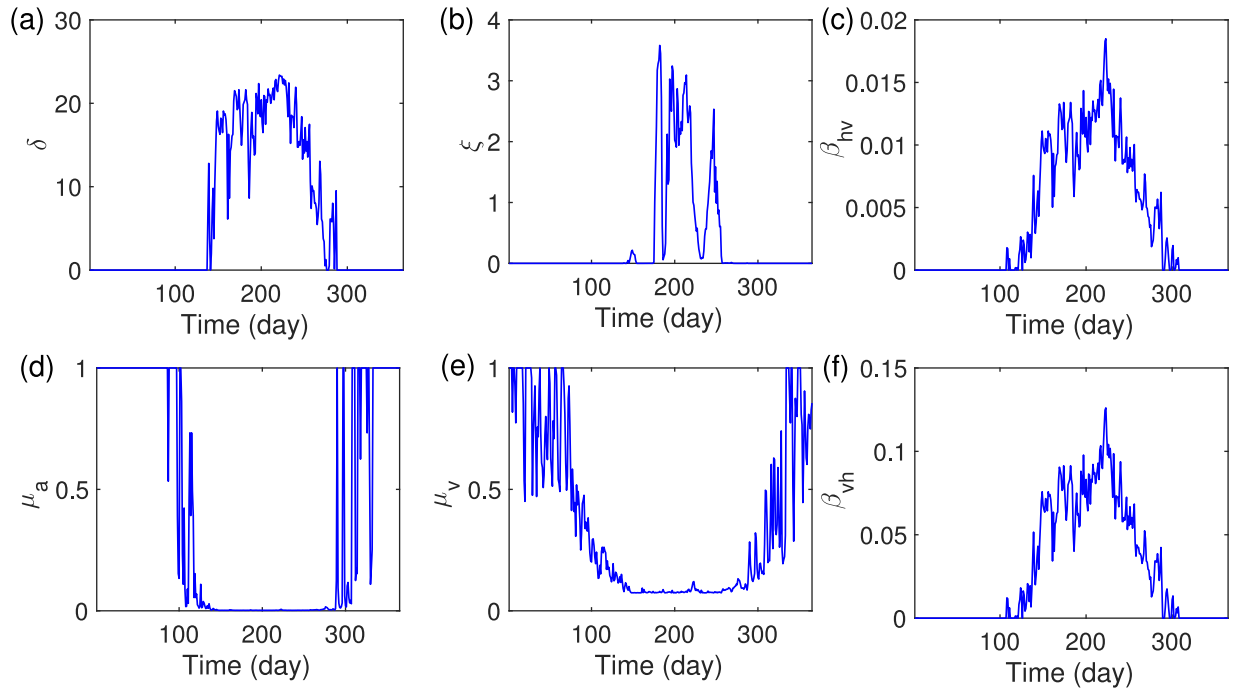

Fig. 11. Daily temperature-dependent parameters are displayed over time based on the RCP 6.0 scenario starting on January 1, 2030: (a) per capita egg deposition rate (δ); (b) maturation rate of immature mosquitoes (ξ); (c) transmissible rate from human to vector (β_{hv}); (d) mortality rate of immature mosquitoes (μ_a); (e) mortality rate of the mosquitoes (μ_v); (f) transmissible rate from vector to human (β_{vh}).

mosquitoes move into the Yeoncheon area through the DMZ from North Korea [16,45]. The simulation results show that a strong control for humans combined with a moderate control of vectors, which is a feasible method of control, effectively reduces the risk of malaria outbreak. Thus, to prevent massive malaria outbreaks, governmental agencies are required to increase budgets and effort to improve their control policies.

One noteworthy characteristic of malaria infection in South Korea is that about 30% of infectious humans in South Korea are military personnel and about 14% are discharged soldiers [27]. Currently in South Korea, most young men in their twenties face mandatory military service for approximately 21 months. As *P. vivax* malaria has a long incubation period of an average of 12 months, if soldiers in long-term latent states become infectious after completing their mandatory military service and returning to the cities where they reside, the risk of massive malaria outbreaks will become high in these cities with the increase of mosquitoes caused by climate change. Thus, a strong and preemptive control approach for areas close to the DMZ with military units such as Yeoncheon is important to reduce the risk of malaria outbreak in South Korea. Moreover, as malaria transmission in the areas close to the DMZ is affected by malaria outbreaks in North Korea [16,46], a possible effective control method to reduce the risk of malaria outbreak in South Korea is to support preventive medicine, insecticide, and other control measures in North Korea.

Acknowledgments

This work was supported by Basic Science Research Program through the National Research Foundation of Korea (NRF) funded by the Ministry of Education (2016R1D1A1B03934427).

Appendix A. Correlation between cumulative malaria incidence and temperature/precipitation

Table 4 shows the relationship between the weekly cumulative incidence of infected mosquitoes and temperature/precipitation based on the RCP scenarios. We use two widely used measures of non-parametric rank correlations: Spearman's ρ and Kendall's τ [47].

One sees that the cumulative incidence has a positive correlation with both of temperature and precipitation.

Table 4
Correlation between weekly cumulative number of infectious mosquitoes and RCP scenarios.

	Spearman		Kendall	
RCP	ρ	p	τ	p
2.6	0.2460	5.7133e−52	0.1504	1.0936e−42
4.5	0.1982	5.7068e−34	0.1233	3.0990e−29
6.0	0.2152	6.7950e−40	0.1349	1.1799e−34
8.5	0.2572	8.7695e−57	0.1635	4.1284e−50

(a) Temperature

	Spearman		Kendall	
RCP	ρ	p	τ	p
2.6	0.3484	1.1401e−105	0.2259	8.4775e−94
4.5	0.3427	4.0650e−102	0.2267	2.3186e−94
6.0	0.3496	1.8856e−106	0.2275	3.6710e−95
8.5	0.4108	3.9894e−150	0.2729	1.6131e−135

(b) Precipitation

Appendix B. Simulation results for $I_h(0) = 1$ in case of no control

In Fig. 12, we display the simulation results of the case of the initial condition $I_h(0) = 1$. Fig. 12 shows the time evolution of incidence and annual cumulative number of infectious mosquitoes and humans for 70 years between 2030 and 2100 when there is no control. Similarly to the case of $I_v(0) = 100$ in Section 3.1, Fig. 12 (a) and (b) show that malaria outbreaks for mosquitoes and humans have recurrent seasonal patterns. Also, Fig. 12 (c) and (d) display that malaria outbreaks will occur on a long time scale.

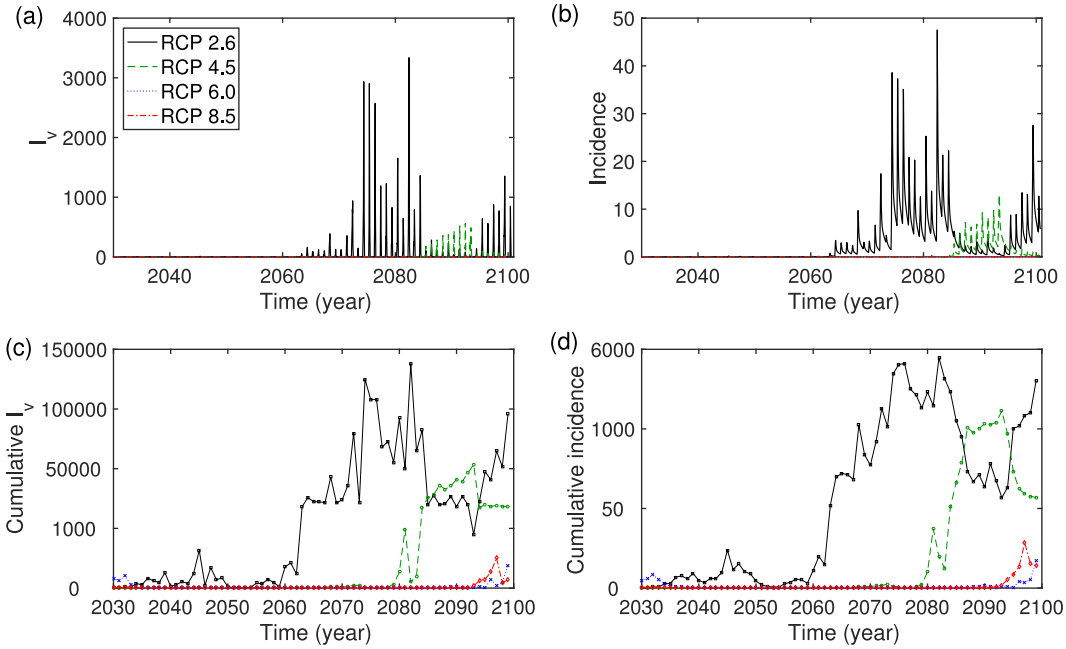

Fig. 12. Incidences of malaria infections in case of no control: Time series of (a) number of infectious mosquitoes and (b) incidence of humans, and annual cumulative number of (c) infectious mosquitoes and (d) incidence of humans are displayed during 70 years based on RCP 2.6 (black solid line), RCP 4.5 (green dashed line), RCP 6.0 (blue dotted line) and RCP 8.5 (red dash-dotted line) with the initial condition $I_h(0) = 1$. (For interpretation of the references to color in this figure legend, the reader is referred to the web version of this article.)

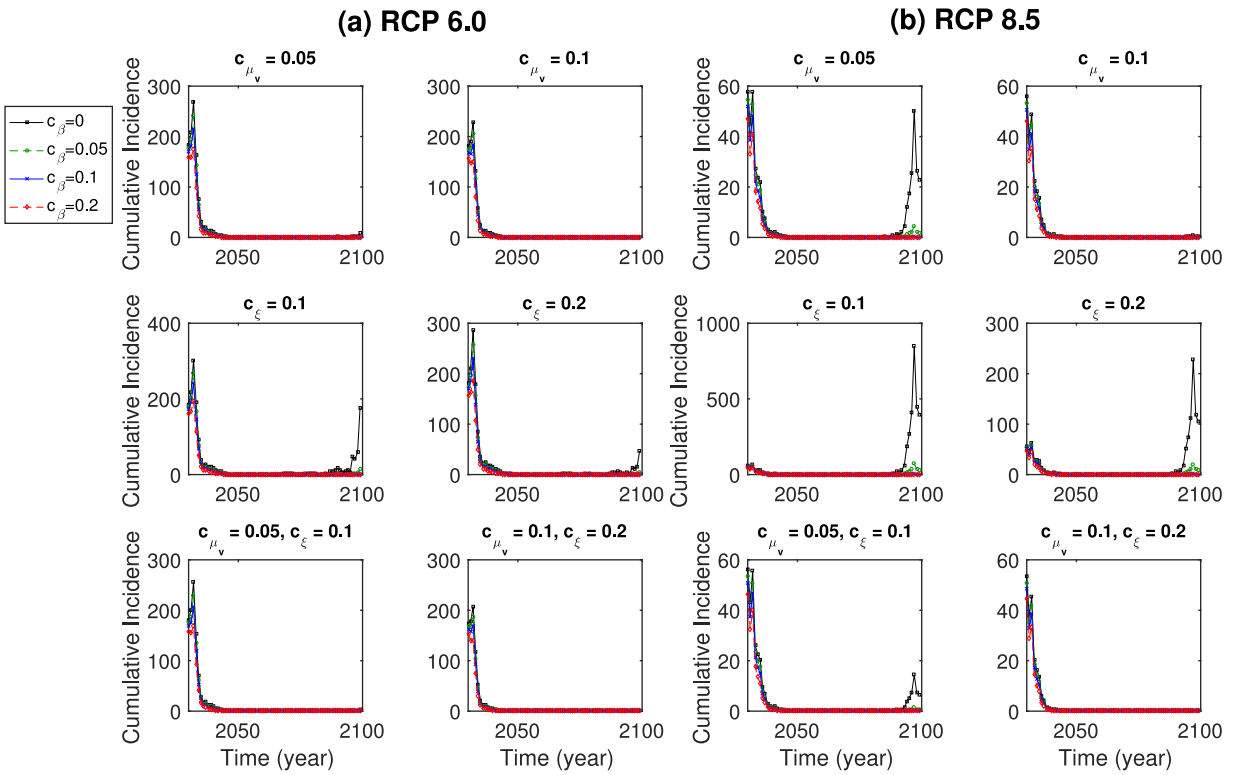

Fig. 13. Combined control effects on yearly cumulative incidence for μ_v (top), ξ (middle) and both (bottom) with control on β under (a) RCP 6.0 and (b) RCP 8.5 for the control threshold $\theta = 10$ with the initial condition $I_v(0) = 100$.

Appendix C. Control effect on cumulative incidence for $I_v(0) = 100$

We consider the control effect on cumulative incidence for the case of the initial condition $I_v(0) = 100$ under RCP 6.0 and 8.5 scenarios. Fig. 13(a) shows that in case of RCP 6.0, despite strong controls, an outbreak may occur between 2030 and 2040, but if strong controls are maintained, there is little risk of outbreak on a long time scale. On the other hand, Fig. 13(b) shows that in case of RCP 8.5, the controls are very effective for the first 60 years; however, the risk of outbreak will increase after the year 2090 unless a strong control is implemented.

References

[1] World Health Organization, World Malaria Report 2017, World Health Organization, 2017.
[2] K. Nah, Y. Kim, J.M. Lee, The dilution effect of the domestic animal population on the transmission of p. vivax malaria, J. Theor. Biol. 266 (2) (2010) 299–306.
[3] D.K. Kochar, A. Das, S.K. Kochar, V. Saxena, P. Sirohi, S. Garg, A. Kochar, M.P. Khatri, V. Gupta, Severe plasmodium vivax malaria: a report on serial cases from bikaner in northwestern india, Am. J. Trop. Med. Hyg. 80 (2) (2009) 194–198.
[4] J.H. Im, H.Y. Kwon, J. Baek, S.W. Park, A. Durey, K.H. Lee, M.-H. Chung, J.-S. Lee, Severe plasmodium vivax infection in korea, Malar. J. 16 (1) (2017) 51.
[5] W. Martens, L.W. Niessen, J. Rotmans, T.H. Jetten, A.J. McMichael, Potential impact of global climate change on malaria risk., Environ. Health Perspect. 103 (5) (1995) 458–464.
[6] S.I. Hay, J. Cox, D.J. Rogers, S.E. Randolph, D.I. Stern, G.D. Shanks, M.F. Myers, R.W. Snow, Climate change and the resurgence of malaria in the east african highlands, Nature 415 (6874) (2002) 905–909.
[7] P.W. Gething, D.L. Smith, A.P. Patil, A.J. Tatem, R.W. Snow, S.I. Hay, Climate change and the global malaria recession, Nature 465 (7296) (2010) 342–345.
[8] C. Caminade, S. Kovats, J. Rocklov, A.M. Tompkins, A.P. Morse, F.J. Colón-González, H. Stenlund, P. Martens, S.J. Lloyd, Impact of climate change on global malaria distribution, Proc. Nat. Acad. Sci. 111 (9) (2014) 3286–3291.
[9] Y.-M. Kim, J.-W. Park, H.-K. Cheong, Estimated effect of climatic variables on the transmission of plasmodium vivax malaria in the republic of korea, Environ. Health Perspect. 120 (9) (2012) 1314.
[10] E.A. Mordecai, K.P. Paaijmans, L.R. Johnson, C. Balzer, T. Ben-Horin, E. Moor, A. McNally, S. Pawar, S.J. Ryan, T.C. Smith, et al., Optimal temperature for malaria transmission is dramatically lower than previously predicted, Ecol. Lett. 16 (1) (2013) 22–30.
[11] A.J. McMichael, R.E. Woodruff, S. Hales, Climate change and human health: present and future risks, The Lancet 367 (9513) (2006) 859–869.
[12] N. Chitnis, J.M. Cushing, J. Hyman, Bifurcation analysis of a mathematical model for malaria transmission, SIAM J. Appl. Math. 67 (1) (2006) 24–45.
[13] T. Bakary, S. Boureima, T. Sado, A mathematical model of malaria transmission in a periodic environment, J. Biol. Dyn. 12 (1) (2018) 400–432.
[14] X. Wang, Y. Chen, S. Liu, Dynamics of an age-structured host-vector model for malaria transmission, Math. Methods Appl. Sci. 41 (5) (2018) 1966–1987.
[15] B.N. Kim, K. Nah, C. Chu, S.U. Ryu, Y.H. Kang, Y. Kim, Optimal control strategy of plasmodium vivax malaria transmission in korea, Osong Public Health Res. Perspect. 3 (3) (2012) 128–136.
[16] M. Noh, Y. Lee, S. Oh, C. Chu, J. Gwack, S.-K. Youn, S.H. Cho, W.J. Lee, S. Huh, Spatial and temporal distribution of plasmodium vivax malaria in korea estimated with a hierarchical generalized linear model, Osong Public Health Res. Perspect. 3 (4) (2012) 192–198.
[17] S. Mandal, R.R. Sarkar, S. Sinha, Mathematical models of malaria-a review, Malaria J. 10 (1) (2011) 202.

[18] P.E. Parham, D. Pople, C. Christiansen-Jucht, S. Lindsay, W. Hinsley, E. Michael, Modeling the role of environmental variables on the population dynamics of the malaria vector anopheles gambiae sensu stricto, Malaria J. 11 (1) (2012) 271.
[19] K.P. Paaijmans, L.J. Cator, M.B. Thomas, Temperature-dependent pre-bloodmeal period and temperature-driven asynchrony between parasite development and mosquito biting rate reduce malaria transmission intensity, PLoS One 8 (1) (2013) e55777.
[20] L.M. Beck-Johnson, W.A. Nelson, K.P. Paaijmans, A.F. Read, M.B. Thomas, O.N. Bjørnstad, The effect of temperature on anopheles mosquito population dynamics and the potential for malaria transmission, PLoS One 8 (11) (2013) e79276.
[21] T.M. Lunde, M.N. Bayoh, B. Lindtjørn, How malaria models relate temperature to malaria transmission, Parasites & Vectors 6 (1) (2013) 20.
[22] K. Okuneye, A.B. Gumel, Analysis of a temperature-and rainfall-dependent model for malaria transmission dynamics, Math. Biosci. 287 (2017) 72–92.
[23] A. Abdelrazec, A.B. Gumel, Mathematical assessment of the role of temperature and rainfall on mosquito population dynamics, J. Math. Biol. 74 (6) (2017) 1351–1395.
[24] L.M. Beck-Johnson, W.A. Nelson, K.P. Paaijmans, A.F. Read, M.B. Thomas, O.N. Bjørnstad, The importance of temperature fluctuations in understanding mosquito population dynamics and malaria risk, R. Soc. Open Sci. 4 (3) (2017) 160969.
[25] S.E. Eikenberry, A.B. Gumel, Mathematical modeling of climate change and malaria transmission dynamics: a historical review, J. Math. Biol. (2018) 1–77.
[26] Intergovernmental Panel on Climate Change (IPCC), in: Fifth assessment report, 2014. (http://www.ipcc.ch/report/ar5/).
[27] Korea Centers for Disease Control and Prevention (KCDC), in: 2017 malaria control manual, 2017. (http://cdc.go.kr/CDC/together/CdcKrTogether0302.jsp?menuIds=HOME001-MNU1154-MNU0725-MNU0088&cid=74549).
[28] Korea Centers for Disease Control and Prevention (KCDC), Mathematical modelling on p.vivax malaria transmission and development of its application program, 2009, (http://www.cdc.go.kr/CDC/eng/).
[29] H. Nishiura, H.-W. Lee, S.-H. Cho, W.-G. Lee, T.-S. In, S.-U. Moon, G.T. Chung, T.-S. Kim, Estimates of short-and long-term incubation periods of plasmodium vivax malaria in the republic of korea, Trans. R. Soc. Trop. Med. Hyg. 101 (4) (2007) 338–343.
[30] Y.-M. Kim, J.-W. Park, H.-K. Cheong, Estimated effect of climatic variables on the transmission of plasmodium vivax malaria in the republic of korea, Environ. Health Perspect. 120 (9) (2012) 1314–1319.
[31] Korea Centers for Disease Control and Prevention (KCDC), Infectious disease statistics system, 2018, (http://is.cdc.go.kr/dstat/index.jsp).
[32] F. Brauer, C. Castillo-Chavez, Mathematical Models in Population Biology and Epidemiology, 1, Springer, 2012.
[33] J.E. Kim, H. Lee, C.H. Lee, S. Lee, Assessment of optimal strategies in a two-patch dengue transmission model with seasonality, PLoS One 12 (3) (2017) e0173673.
[34] Korea Global Atmosphere Watch Center(KGAWC), 2017, (http://www.climate.go.kr/).
[35] F. Chamchod, J.C. Beier, Modeling plasmodium vivax: relapses, treatment, seasonality, and g6pd deficiency, J. Theor. Biol. 316 (2013) 25–34.
[36] P.E. Parham, E. Michael, Modeling the effects of weather and climate change on malaria transmission, Environ. Health Perspect. 118 (5) (2010) 620–626.
[37] A. Tran, G. L'Ambert, G. Lacour, R. Benoît, M. Demarchi, M. Cros, P. Cailly, M. Aubry-Kientz, T. Balenghien, P. Ezanno, A rainfall-and temperature-driven abundance model for aedes albopictus populations, Int. J. Environ. Res. Public Health 10 (5) (2013) 1698–1719.
[38] Korean Statistical Information Service(KOSIS), in: Population projections and summary indicators(province), 2017. (http://kosis.kr/eng/statisticsList/).
[39] S.-C. Chen, M.-H. Hsieh, Modeling the transmission dynamics of dengue fever: implications of temperature effects, Sci. Total Environ. 431 (2012) 385–391.
[40] C. Garrett-Jones, Prognosis for interruption of malaria transmission through assessment of the mosquito's vectorial capacity, Nature 204 (4964) (1964) 1173–1175.
[41] Y.A. Afrane, T.J. Little, B.W. Lawson, A.K. Githeko, G. Yan, Deforestation and vectorial capacity of anopheles gambiae giles mosquitoes in malaria transmission, kenya, Emerg. Infect. Dis. 14 (10) (2008) 1533–1538.
[42] K.P. Paaijmans, S. Blanford, B.H. Chan, M.B. Thomas, Warmer temperatures reduce the vectorial capacity of malaria mosquitoes, Biol. Lett. 8 (3) (2011) 465–468. rsbl20111075.
[43] R. Anderson, R. May, Infectious Diseases of Humans: Dynamics and Control, Oxford University Press, 1992.
[44] N. Chitnis, J.M. Hyman, J.M. Cushing, Determining important parameters in the spread of malaria through the sensitivity analysis of a mathematical model, Bull. Math. Biol. 70 (5) (2008) 1272–1296.
[45] D.H. Foley, T.A. Klein, H.C. Kim, W.J. Sames, R.C. Wilkerson, L.M. Rueda, Geographic distribution and ecology of potential malaria vectors in the republic of korea, J. Med. Entomol. 46 (3) (2009) 680–692.
[46] M. Iwagami, M. Fukumoto, S.-Y. Hwang, S.-H. Kim, W.-G. Kho, S. Kano, Population structure and transmission dynamics of plasmodium vivax in the republic of korea based on microsatellite dna analysis, PLoS Negl. Tropical Dis. 6 (4) (2012) e1592.
[47] M. Hollander, D.A. Wolfe, E. Chicken, Nonparametric Statistical Methods, 751, John Wiley & Sons, 2013.